Structural Response Assessment of High-Rise Buildings Subjected to Wind Loads Considering the Brazilian Standard and CFD Simulations

George Lucas da Silva Quintanilha
Postgraduate Program in Civil Engineering, Rio de Janeiro State University, Brazil
eng.georgequintanilha@gmail.com

Leonardo Ferreira de Miranda
Postgraduate Program in Civil Engineering, Rio de Janeiro State University, Brazil
leonardofm.eng@gmail.com

Jose Guilherme Santos da Silva
Postgraduate Program in Civil Engineering, Rio de Janeiro State University, Brazil
jgss@uerj.br (corresponding author)

Received: 25 January 2026 | Revised: 22 March 2026 | Accepted: 1 April 2026

 DOI: https://doi.org/10.48084/etasr.17752

ABSTRACT

This study examines human comfort in tall buildings subjected to non-deterministic wind loads, considering different analysis methodologies and design recommendations. Since wind velocity is composed of a mean component and a fluctuating component, the mean part was determined in accordance with the recommendations of the Brazilian standard NBR 6123 and through numerical simulation based on Computational Fluid Dynamics (CFD) analysis, whereas the fluctuating part was defined using the Spectral Representation Method (SRM). The case study comprises a 100 m high reinforced concrete building, for which numerical analysis was performed using the Finite Element Method (FEM) in the ANSYS software. The results indicated that the variation in dynamic responses between the methodologies reached 10% for displacements and 5% for accelerations. Maximum displacements and RMS accelerations satisfied the adopted limits. However, peak accelerations exceeded the comfort requirements for residential buildings.

Keywords-wind loads; high-rise buildings; human comfort assessment; Computational Fluid Dynamics (CFD)

I. INTRODUCTION

The development of high-rise buildings constitutes a solution for accommodating high population densities within restricted urban spaces. However, these structures exhibit lower natural frequencies, rendering them more susceptible to excessive vibration under wind loads [1]. This dynamic behavior can cause occupant discomfort, highlighting the need to investigate the stochastic dynamic response of buildings, concerning human comfort levels [1, 2].

The wind exhibits inherently unstable characteristics, resulting in stochastic load distributions; consequently, adopting a deterministic approach to this phenomenon is inadequate [3]. According to NBR 6123 [4], wind velocity consists of two distinct components. The first component represents the mean velocity, which induces exclusively static effects on the structure. In contrast, the second component corresponds to the fluctuating response, which generates oscillations in the same direction as the mean response and exhibits a non-deterministic nature.

Despite widespread application, NBR 6123 employs a simplified procedure for determining dynamic pressure variation with height, predicated on constant cross-sections and uniform mass distribution. Due to its inherent simplification, this approach yields purely static loading conditions. The present investigation proposes a hybrid framework in which NBR 6123 is applied exclusively to compute the mean wind component, while the fluctuating component is derived using the Spectral Representation Method (SRM). By this procedure, stochastic time-series loading data are generated, thereby enabling transient dynamic analysis and facilitating response evaluation conducted in both time and frequency domains. Similarly, the Brazilian standard proposes a single drag coefficient based on nomograms for wind load determination on structural systems with constant cross-section.

Computational Fluid Dynamics (CFD) [5] is often used for analyzing the complex geometric configurations by mapping wind-induced aerodynamic effects around structural systems and determining pressure coefficient distributions across building facades [6]. Therefore, CFD analysis is also adopted in the definition of the mean wind component, with the resulting pressure coefficients applied in the dynamic load definition, while the fluctuating component remains determined by the SRM. Finally, the results are compared with each other and with the prescribed assessment limits.

This study investigates the non-deterministic dynamic structural response and assesses human comfort in a 30-storey reinforced concrete building with a total height of 100 m. The numerical model was developed using discretization techniques based on the Finite Element Method (FEM), implemented in the ANSYS Mechanical software (2019) [7]. The comparative analysis revealed differences of up to 10% for displacements and 5% for accelerations in the dynamic responses, potentially compromising the structure's conformity with normative limits. Compliance with the specified limits was observed for maximum horizontal displacements (u_{lim} = 0.059 m) and RMS accelerations (a_{rmslim} = 0.032 m/s²), while peak accelerations failed to meet the comfort requirements applicable to residential buildings (a_{lim} = 0.072 m/s²).

II. BRAZILIAN STANDARD NBR 6123 GUIDELINES

Following the recommendations of the Brazilian standard NBR 6123 [4], the definition of the wind velocity profile corresponding to the static component is based on the characteristic wind velocity, as expressed in (1). The basic wind velocity, V_0, measured in m/s, is established according to the geographical region of the structure. The factor S_1 represents a topographic factor predicated on variations in terrain relief. The factor S_2, as defined by (2), incorporates the effects of terrain roughness, wind velocity variation along the structure height, and the building dimensions. Furthermore, the probabilistic factor S_3 considers a return period and return probability, which is 0.54 when assessing human comfort. Table I summarizes the parameters utilized in this research work:

$$\bar{V}(z) = V_0 S_1 S_2 S_3 \quad (1)$$

$$S_2 = bF_r \left(\frac{z}{10}\right)^p \quad (2)$$

TABLE I. WIND VELOCITY PARAMETERS

Parameters		Description	Value
V_0		Basic wind speed	45 m/s
S_1		Topographic factor	1
S_2	b	Meteorological parameter	0.71
	Fr	Gust factor	0.69
	p	Exponent of the potential law	0.23
	z	Height above the terrain (in meters)	Variable
S_3		probabilistic factor	0.54

In addition to the guidelines for determining the static component of wind, NBR 6123 [4] also establishes recommendations for defining wind loads, considering the dynamic pressure, the building geometry, and the drag coefficient. The drag coefficient represents a correlation among all points on the building façade exposed to wind action, while the reference velocity $\bar{V}(z)$ varies with height. This parameter is obtained from abacuses provided in the standard.

III. NUMERICAL SIMULATION

The analysis of wind behavior through CFD [5] remains a critical aspect of engineering, as most fluid flows exhibit turbulence and are characterized by chaotic, irregular, and unpredictable patterns [8]. Turbulent flows are inherently unstable, three-dimensionally complex, and time-dependent. Furthermore, viscosity exhibits non-linear and unpredictable characteristics. Therefore, the formulation of methodologies to ensure the comprehensive definition and implementation of governing viscous equations is essential.

Numerous turbulence models are documented in the literature, necessitating a rigorous selection process for specific engineering applications. Considering the ANSYS Fluent software environment [5], the standard $k-\epsilon$ model is often utilized. This turbulence model provides reliable results and is particularly suited for fully developed turbulent flows. Additionally, relatively low computational effort is required compared to alternative models [9]. The $k-\epsilon$ turbulence model belongs to the class of two-equation models, where velocity and length scales are determined through the solution of two transport equations. The variable k represents the turbulent kinetic energy, while ϵ represents the dissipation rate. Extensive application of this model in fluid flow simulations is attributed to its robustness, computational efficiency, and satisfactory accuracy across a broad spectrum of turbulence-related flow scenarios.

Inherent limitations exist despite the standard $k-\epsilon$ model's widespread utilization. Modifications were introduced to enhance overall performance as technical strengths and deficiencies were more comprehensively identified. Consequently, various refined versions of the model were developed, with several available in ANSYS Fluent software [5]. An alternative model is the Renormalization Group Theory (RNG)-$k-\epsilon$ employed as the turbulence model for the CFD simulations conducted in this study. This model is derived through a rigorous statistical approach known as RNG. Although structurally analogous to the Standard $k-\epsilon$ model, the RNG $k-\epsilon$ model incorporates refinements that improve accuracy and reliability across various flow conditions. More information is available at the ANSYS Fluent User Guide [5].

The analytical definition of the initial conditions for a horizontally homogeneous atmospheric boundary layer is achieved by solving the turbulence model in conjunction with wall-function equations under equilibrium conditions. Richards and Hoxey [10] formulated the velocity profile via a logarithmic equation, as presented in (3), alongside the corresponding turbulence kinetic energy (k) and dissipation rate (ϵ) profiles, represented as:

$$\bar{V}(z) = \frac{u_*}{\kappa} ln\left(\frac{z+z_0}{z_0}\right) \quad (3)$$

$$k = \frac{u_*^2}{\sqrt{C_\mu}} \quad (4)$$

$$\epsilon = \frac{u_*^3}{\kappa(z+z_0)} \quad (5)$$

where the friction velocity u_* within the atmospheric boundary layer is taken as 2.98 m/s. A roughness length z_0 of 2 m is adopted, corresponding to a densely developed urban environment characterized by the presence of high-rise structures [11]. The von Karman constant k is specified as 0.4, whereas the empirical constant C_μ is defined as 0.085.

Regarding the solver configuration, pseudo-transient analyses were performed utilizing a pressure-velocity coupling method with a coupled scheme. The spatial discretization for the gradient calculation employed the Green-Gauss node-based approach, while second-order schemes were applied to the pressure, momentum, turbulent kinetic energy, and turbulent dissipation rate equations. Upon defining all necessary parameters, the subsequent step consists of inputting the velocity profile. Due to its logarithmic formulation, direct insertion is not feasible; therefore, implementation is carried out through a User Defined Function (UDF). Finally, pressure monitors were positioned on the building facades.

The analysis results include the pressure coefficient values obtained at various points on the building facades, based on a reference velocity calculated at the highest point of the structure. These coefficients are employed in the computation of non-deterministic wind loads.

IV. MATHEMATICAL MODELING OF THE NON-DETERMINISTIC LOADS

The proposed methodologies, are associated with the static component of the wind. However, the wind exhibits a non-deterministic dynamic behavior. Consequently, the fluctuating component $\hat{V}(z,t)$ must also be accounted for in addition to the static component $\bar{V}(z)$. This relationship is expressed in (6), where $\hat{V}(z,t)$ represents the non-deterministic wind velocity:

$$V(z,t) = \bar{V}(z) + \hat{V}(z,t) \quad (6)$$

The non-deterministic component is represented by a finite number of harmonic functions, considering the random phase angles [12]. According to [14], signals exhibiting these characteristics can be determined through the SRM, which utilizes the Power Spectral Density (PSD) function of the signal to derive the amplitudes and frequencies of each harmonic. Equation (7) demonstrates the application of the SRM in defining the fluctuating component of the wind, where $S^v(f_i)$ denotes the spectral density, Δf represents the frequency increment, f_i corresponds to the frequency of each harmonic i, and θ_i signifies the random phase angle defined within the interval from 0 to 2π:

$$\hat{V}(z,t) = \sum_{i=1}^{N} \sqrt{2S^v(f_i)\Delta f}\cos(2\pi f_i t + \theta_i) \quad (7)$$

The amplitude of each harmonic is determined based on the spectral density $S^v(f_i)$, with the Kaimal power spectrum adopted in this study due to its formulations incorporating building height, as presented in (8) and (9). The variable X denotes the dimensionless frequency, while u_* represents the friction velocity, calculated using (10). Additionally, K is defined as the Karman constant, $\bar{V}(z)$ corresponds to the static component of the wind velocity, z_0 represents the roughness length in m, and z is the height in m:

$$\frac{fS(f,Z)}{{u_*}^2} = \frac{200X}{(1+50X)^{5/3}} \quad (8)$$

$$X(f,Z) = \frac{fZ}{\bar{V}(Z)} \quad (9)$$

$$u_* = \frac{K\bar{V}(Z)}{ln\left(\frac{Z}{Z_0}\right)} \quad (10)$$

Considering both the static and fluctuating components of wind velocity, the non-deterministic dynamic loading can be defined. The parameter A_i is the tributary area in m², while ρ is the air density (ρ = 1.225 kg/m³), and $V_i(z,t)$ represents the non-deterministic velocity. The non-deterministic dynamic loads can be calculated as:

$$F(z,t) = \frac{1}{2}\rho V_i(z,t)^2 A_i C_p \quad (11)$$

V. STRUCTURAL AND FINITE ELEMENT MODEL

The investigated structural model consists of a 30-storey reinforced concrete building with a total height of 100 m. The floor plan of the building is presented in Figure 1. The structure is composed of columns, beams, and slabs. The concrete has a compressive strength (f_{ck}) of 25 MPa, a secant modulus of elasticity (E_{cs}) of 24 GPa, a Poisson's ratio (ν) of 0.2, and a density (ρ) of 2500 kg/m³.

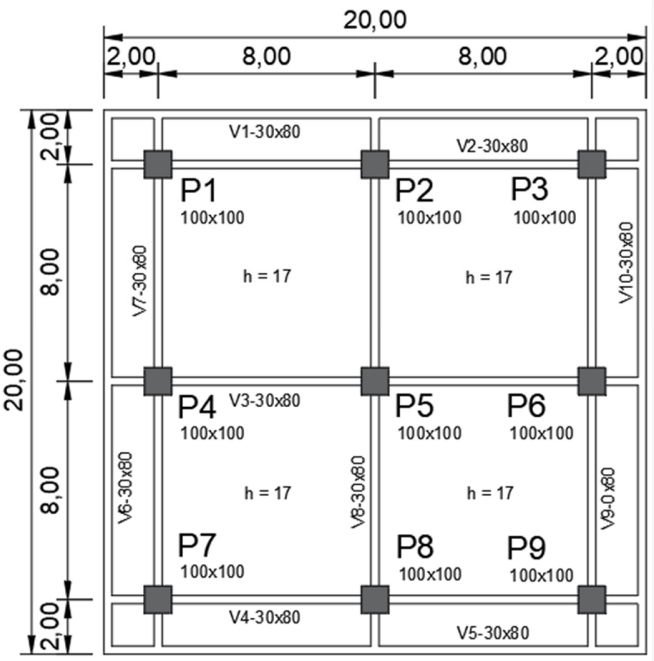

Fig. 1. Floor plan of the analyzed building.

The structural system was modeled using the ANSYS software [7], based on FEM. The modeling of columns and beams was performed using BEAM44 elements, which incorporate the effects of bending and torsion. The slabs were represented by SHELL63 elements. The former were subdivided into square elements with a side length of 25 cm,

while the columns and beams were segmented linearly into elements of 50 cm and 25 cm, respectively. Translational displacements were constrained at the column bases, and the structural elements were assumed to be rigidly connected.

The numerical model was subjected to a series of convergence tests to determine an adequate level of refinement, ensuring an accurate representation of the dynamic behavior of the structure. Considering the mechanical properties of the reinforced concrete, the model was considered isotropic and linear-elastic. Figure 2 illustrates the finite element representations of the analyzed building.

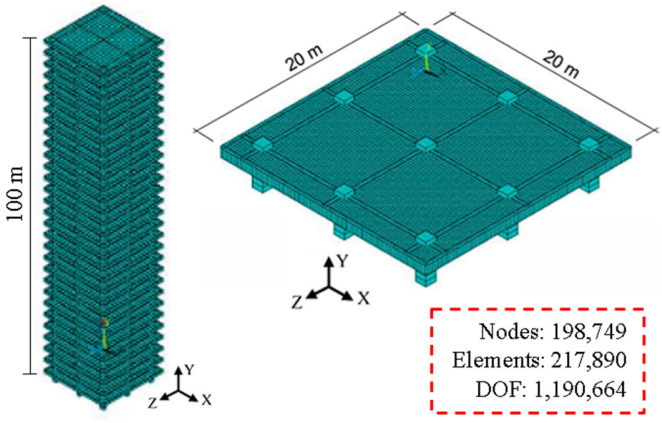

Fig. 2. Finite element model of the analyzed building.

VI. MODAL ANALYSIS: EIGENVALUES AND EIGENVECTORS

Free vibration analyses were performed to obtain the natural frequencies (eigenvalues) and vibration modes (eigenvectors), using the ANSYS software [7]. Figure 3 presents the first four natural frequencies and vibration modes of the analyzed model, illustrating the susceptibility of the structure to vibrations and highlighting the maximum and minimum modal amplitudes.

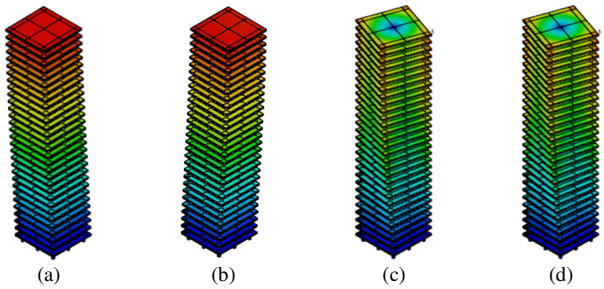

Fig. 3. Natural frequencies and vibration modes: (a) f_{01} = 0.277 Hz bending around the X-axis, (b) f_{02} = 0.278 Hz bending around the Z-axis, (c) f_{03} = 0.372 Hz torsion around the Y-axis, and (d) f_{04} = 0.882 Hz bending around the Z-axis.

The results indicate a predominant vibration mode associated with the bending effect. As the building exhibits the same inertia in both principal directions, the first and second natural frequencies present similar values (f_{01} = 0.277 Hz and f_{02} = 0.278 Hz). Furthermore, buildings with a natural frequency below 1 Hz are susceptible to excessive vibrations [4]. This condition indicates that the modal amplitudes are relevant due to the high flexibility of the structural model.

VII. TRANSIENT ANALYSIS: NBR 6123 AND CFD

Based on the above methodologies, the maximum horizontal displacements and accelerations of the structure were determined. The primary results, obtained in the time domain, were subsequently processed using the Fast Fourier Transform (FFT) to derive the corresponding frequency-domain, thereby enabling the identification of energy transfer peaks. This analytical approach enables the assessment of human comfort levels and allows for a comparison between the adopted methodologies under different loading configurations, including wind incidence in both the X- and Z-directions.

Initially, the non-deterministic wind loads were obtained in accordance with the recommendations of the NBR 6123 [4] and the SRM. As a result, 60 load series were generated, comprising 30 series associated with wind acting in the X-direction and 30 corresponding to wind acting in the Z-direction. Subsequently, transient analyses were conducted for each series using the ANSYS software [7]. The parameters utilized in the analysis and the drag coefficients are presented in Table II [4], while Figure 4 shows the result of one of the series in both the time and frequency domains [4].

TABLE II. ANALYSIS PARAMETERS IN ACCORDANCE WITH NBR 6123 [4]

Parameters	Value
Initial frequency	0.00167 Hz
Final frequency	5 Hz
Frequency increase	0.00167 Hz
Initial time	0s
Final time	600s
Time increment	0.1s
Drag coefficients	1.39

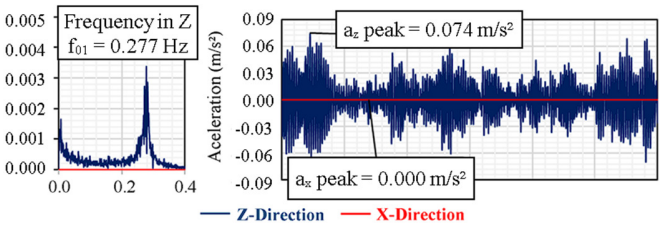

Fig. 4. Acceleration in the time and frequency domains based on NBR 6123 [4].

The dynamic responses were analyzed using statistical procedures based on the mean and standard deviation of the collected data, ensuring a 95% confidence level of the characteristic response [13]. Accordingly, the characteristic peak displacement, peak acceleration, and RMS acceleration were determined. Table III summarizes the computed results [4]. The second analysis method adopted was a simulation based on CFD analysis. Following the procedure described in Section III, the computational domain was defined around the building model to replicate wind tunnel flow conditions [14], and the dimensions were determined in accordance with the

criteria proposed in [15]. Therefore, the domain presents a width of 410 m, a depth of 650 m, and a height of 415 m. The building was positioned 150 m from the inlet face and 195 m from the lateral boundaries to ensure appropriate flow development.

TABLE III. BUILDING DYNAMIC RESPONSE IN ACCORDANCE WITH NBR 6123 [4]

Parameters	X direction		Z direction	
	Wind in Z	Wind in X	Wind in Z	Wind in X
Peak displacement (m)	0.000	0.041	0.029	0.011
Peak acceleration (m/s²)	0.000	0.080	0.080	0.001
RMS acceleration (m/s²)	0.000	0.021	0.021	0.000

Hexahedral (hex-dominant) elements with different mesh sizes were used for model discretization. Finer elements (1.0 × 1.665 m) were applied on the building faces, while larger elements were used toward the domain boundaries, with a maximum size of 6 m and a growth rate of 1.05 to ensure a smooth transition. Element sizes were defined considering the location of pressure monitors on the building facades, aligning them with mesh nodes to allow wind pressure evaluation. Following a mesh independence study, which showed a 0.60% difference in wind gust compared to the analytical calculation, the final mesh consisted of 887,472 elements.

During the analyses, the residual convergence threshold and the time-step adopted in the pseudo-transient solver were defined as 10^{-3} and from 0.5 to 3, respectively. Moreover, the windward and leeward pressures were monitored in order to verify the convergence of the results, which was achieved after 1,715 iterations, yielding a windward pressure of 392.22 Pa and a leeward pressure of −222.69 Pa. The results consist of the pressure coefficient values obtained at each pressure monitor on the building facades, as well as contour plots illustrating the pressure distribution and the wind flow behavior around the structure. Figures 5 and 6 display the contour plots considering the wind action in the Z-direction.

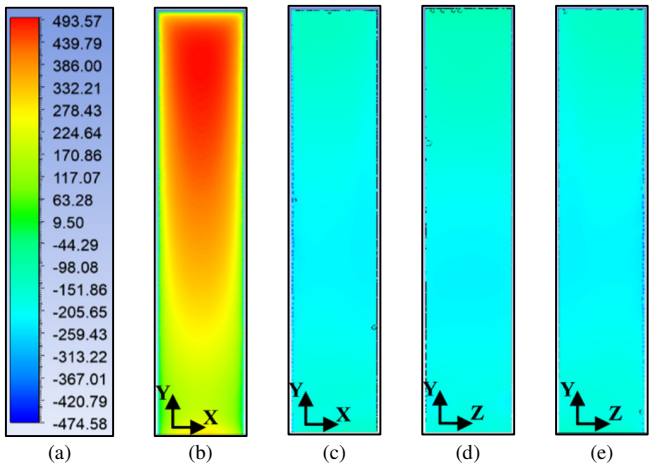

Fig. 5. CFD analysis results with pressure contour plots in Z-direction: (a) pressure (Pa), (b) windward, (c) leeward, (d) left facade, (e) right facade.

Considering the pressure coefficient values obtained through the pressure monitors and using the SRM, 60 dynamic loading time series were generated. Among these series, 30 correspond to wind action in the X-direction, whereas the remaining 30 are associated with the Z-direction. Transient analyses were performed in ANSYS software [7], in which the number and location of the pressure monitors define the points of the load vectors applied for each series. Figure 6 depicts the results of a time-domain and frequency-domain series, while Table IV presents, after statistical treatment, the characteristic values of the peak displacement, the peak acceleration, and the RMS acceleration.

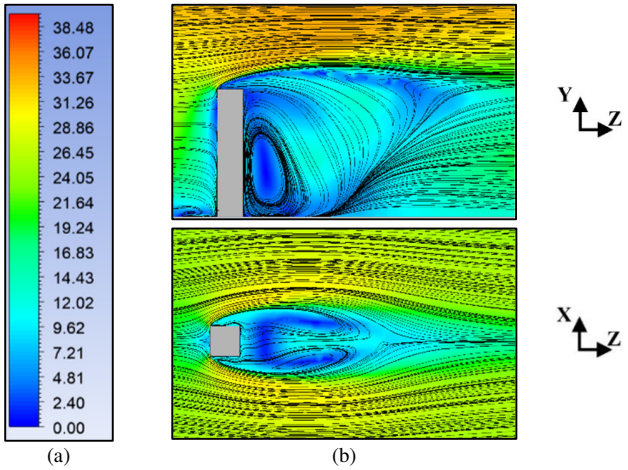

Fig. 6. CFD analysis results with wind velocity contour plots in Z-direction: (a) wind velocity (m/s), (b) wind direction: left to right.

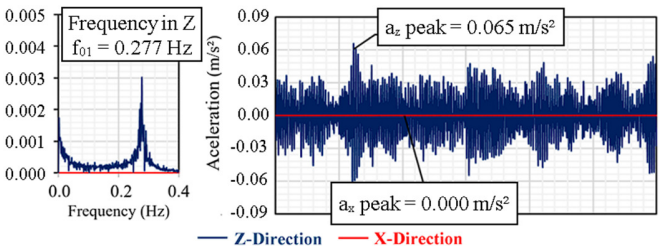

Fig. 7. CFD analysis results: acceleration in the time and frequency domains.

TABLE IV. BUILDING DYNAMIC RESPONSE

Parameters	X direction		Z direction	
	Wind in Z	Wind in X	Wind in Z	Wind in X
Peak displacement (m)	0.000	0.038	0.026	0.011
Peak acceleration (m/s²)	0.000	0.079	0.083	0.000
RMS acceleration (m/s²)	0.000	0.021	0.022	0.000

Based on the results, the assessment of human comfort can be performed. Concerning the allowable displacements in the serviceability limit state, the Brazilian standard NBR 6118 [16] specifies that the maximum displacement at the top of the structure should not exceed the limit of H/1700. Addressing accelerations, perception limits have been established based on global population sensitivity. These criteria define limits that may be exceeded within a specific return period. In Brazil,

NBR 6123 [4] proposes that the return period is one year, following the recommendations of the ISO 10137 [17], where the limit acceleration values are calculated as given in (12), where the k_c value of 4.08 is applicable for residential buildings and 6.12 for office buildings, with f representing the fundamental frequency. Nevertheless, regarding RMS acceleration, ISO 6897 [18] presents curve limits considering a return period of at least 5 years, which can be adjusted for a 1-year return period.

$$a_{lim} = 0.01 k_c f^{-0.445} \quad (12)$$

A comparison between the structural response and the adopted limits is provided in Tables V-VII, where both methods provide similar results. Regarding the maximum displacements, the CFD method [5] presents lower values than those obtained using the NBR 6123 [4], with a Δu of −7.32% in the X-direction and a Δu of −10.34% in Z-direction. Considering the acceleration results, both peak and RMS values obtained from the CFD simulation [5] are close to those provided by NBR 6123 [4], with slight variations (Peak: Δa% = −1.25% to +3.75%; RMS: Δa% = −0.47% to +4.76%).

TABLE V. PEAK DISPLACEMENT ASSESSMENT

Method	Peak displacement (m)		NBR 6118 limit (u_{lim} = 0.059 m)
	X	Z	
NBR 6123	0.041 (RV)	0.029 (RV)	Acceptable
CFD	0.038 (-7.32%)	0.026 (-10.34%)	Acceptable

TABLE VI. PEAK ACCELERATION ASSESSMENT

Method	Peak acceleration (m/s²)		NBR 6123 (a_{lim})	
	X	Z	Residential (0.072 m/s²)	Office (0.108 m/s²)
NBR 6123	0.080 (RV)	0.080 (RV)	Not acceptable	Acceptable
CFD	0.079 (-1.25%)	0.083 (+3.75%)	Not acceptable	Acceptable

TABLE VII. RMS ACCELERATION ASSESSMENT

Method	RMS acceleration (m/s²)		ISO 6897 Limit (a_{RMSlim} = 0.032 m/s²)
	X	Z	
NBR 6123	0.021 (RV)	0.021 (RV)	Acceptable
CFD	0.021(-0.47%)	0.022 (+4.76%)	Acceptable

Regarding the displacement limits established by the standard NBR 6118 [20] (u_{lim} = 0.059 m), the values remain within the specified limit. Considering peak acceleration (a = 0.08 m/s² in X-direction and a = 0.08 m/s² in Z-direction), the results obtained from both methods surpassed the limit for residential buildings (a_{lim} = 0.072 m/s²); however, the limit for office buildings was acceptable (a_{lim} = 0.108 m/s²). Finally, the RMS accelerations were below the limits established by the standard ISO 6897 [22] (a_{RMSlim} = 0.032 m/s²).

VIII. CONCLUSION

The current study examined the structural response of a tall building under wind action, based on a multi-approach analytical framework. The methodologies applied were the recommendations of the Brazilian standard NBR 6123 and numerical simulations using Computational Fluid Dynamics (CFD). Based on the analysis, the following conclusions are drawn for the reinforced concrete building under investigation.

- Considering the NBR 6123 method as the reference criterion, the CFD simulations exhibited variations of approximately 10% for displacements and 5% for acceleration values. These percentage differences become meaningful when the building's dynamic structural responses are near the normative thresholds.
- Considering the results in the time and frequency domains, it is observed that only responses in the along-wind direction exhibited significant values. The energy transfer peak was associated with the bending vibration mode (f_{01} = 0.28 Hz).
- Regarding the CFD simulation, the assessment of the contour plots indicates an increase in wind-induced pressure as a function of height variation. Furthermore, the formation of a low-pressure region on the leeward facade is also observed.
- The structural responses obtained in accordance with the NBR 6123 were satisfactory when compared with the CFD-based methodology. Therefore, both methods are suitable for assessing human comfort, provided that wind action is considered as a dynamic, non-deterministic load.

DECLARATION OF COMPETING INTERESTS

The authors declare that they have no known competing interests or personal relationships that could have appeared to influence the work reported in this paper.

ACKNOWLEDGMENTS

The authors gratefully acknowledge the financial support for this study provided by the Brazilian Science Foundation's CAPES, CNPq, and FAPERJ.

DATA AVAILABILITY

The data that support the findings of this study are available from the corresponding author upon reasonable request.

REFERENCES

[1] G. L. S. Quintanilha, "Analysis of the Non-Deterministic Dynamic Structural Behaviour and Assessment of Human Comfort in Tall Buildings When Subjected to Wind Actions Through the Use of Different Analysis Methodologies," Ph.D. Dissertation, Rio de Janeiro State University, Rio de Janeiro, Brazil, 2026.

[2] L. F. Miranda, "Study of the Dynamic Structural Behaviour of High-Rise Buildings When Subjected to Non-Deterministic Wind Actions Considering Pressure Coefficients Based on the Use of Different Strategies," Ph.D. Dissertation, Rio de Janeiro State University, Rio de Janeiro, Brazil, 2026.

[3] J. C. Mota Silva and J. G. Santos da Silva, "Assessment of Building Nondeterministic Dynamic Structural Behavior Considering the Effect of Geometric Nonlinearity and Aerodynamic Damping," *Engineering, Technology & Applied Science Research*, vol. 14, no. 6, pp. 18835–18842, Dec. 2024, https://doi.org/10.48084/etasr.8743.

[4] *Forças Devidas ao Vento em Edificações*, NBR 6123, Associação Brasileira de Normas Técnicas, Rio de Janeiro, Brazil, 2023.

[5] *ANSYS Fluent User's Guide v19.2*. Canonsburg, PA, USA: Ansys Inc., 2019.

[6] D. Sharma, S. Pal, and R. Raj, "CFD Simulation of Wind Effects on Cylindrical Roof of T-Plan Multi-span Low-Rise Building," in *Advances in Construction Management*, vol. 601, A. Kashyap, R. Goyal, R. Y. M. Li, G. Mahesh, and M. D. Deepak, Eds. Singapore: Springer Nature Singapore, 2025, pp. 17–25.

[7] *ANSYS Mechanical APDL*, Ansys Inc., 2019, [Online]. Available: https://www.ansys.com/products/structures/ansys-mechanical.

[8] M. T. Asyikin, "CFD Simulation of Vortex Induced Vibration of a Cylindrical Structure," Ph.D. Dissertation, Institutt for Bygg, Anlegg og Transport, Trondheim, Norway, 2012.

[9] B. E. Launder and D. B. Spalding, "The Numerical Computation of Turbulent Flows," *Computer Methods in Applied Mechanics and Engineering*, vol. 3, no. 2, pp. 269–289, Mar. 1974, https://doi.org/10.1016/0045-7825(74)90029-2.

[10] P. J. Richards and R. P. Hoxey, "Appropriate Boundary Conditions for Computational Wind Engineering Models Using the k-ϵ Turbulence Model," *Journal of Wind Engineering and Industrial Aerodynamics*, vol. 46–47, pp. 145–153, Aug. 1993, https://doi.org/10.1016/0167-6105(93)90124-7.

[11] B. Blocken, "Computational Fluid Dynamics for Urban Physics: Importance, Scales, Possibilities, Limitations and Ten Tips and Tricks Towards Accurate and Reliable Simulations," *Building and Environment*, vol. 91, pp. 219–245, Sep. 2015, https://doi.org/10.1016/j.buildenv.2015.02.015.

[12] M. Shinozuka and C.-M. Jan, "Digital Simulation of Random Processes and Its Applications," *Journal of Sound and Vibration*, vol. 25, no. 1, pp. 111–128, Nov. 1972, https://doi.org/10.1016/0022-460X(72)90600-1.

[13] E. S. Chávez, "Structural Analysis of a High-Rise Building Subjected to Fluctuating Pressures Induced by Wind Action," MSc thesis, School of Engineering, Federal University of Minas Gerais, Belo Horizonte, MG, Brazil, 2006.

[14] D. Sharma, R. Raj, and S. Pal, "Effects of Roof Shapes on Wind Pressure Distribution of Multi-Span Low-Rise Buildings," *Proceedings of International Structural Engineering and Construction*, vol. 10, no. 1, Aug. 2023, https://doi.org/10.14455/ISEC.2023.10(1).STR-19.

[15] J. Liu and J. Niu, "CFD Simulation of the Wind Environment Around an Isolated High-Rise Building: An Evaluation of SRANS, LES and DES Models," *Building and Environment*, vol. 96, pp. 91–106, Feb. 2016, https://doi.org/10.1016/j.buildenv.2015.11.007.

[16] *Projeto de Estruturas de Concreto*, NBR 6118, Associação Brasileira de Normas Técnicas, Rio de Janeiro, RJ, Brazil, 2023.

[17] *Bases for Design of Structures - Serviceability of Buildings and Walkways Against Vibrations*, ISO 10137, International Organization for Standardization, Geneva, Switzerland, 2007.

[18] Guidelines for the Evaluation of Response of Occupants of Fixed Structures, Especially Buildings and Off-Shore Structures to Low-Frequency Horizontal Motion (0.063 to 1 Hz), ISO 6897, International Organization for Standardization, Geneva, Switzerland, 1984.